

# Preparation of activated carbon from kenaf by activation with H<sub>3</sub>PO<sub>4</sub>. Kinetic study of the adsorption/electroadsorption using a system of supports designed in 3D, for environmental applications

A. Macías-García<sup>1</sup>, J. P. Carrasco-Amador<sup>2</sup>, V. Encinas-Sánchez<sup>3</sup>, M.A. Díaz-Díez<sup>1</sup>, D.  
Torrejón-Martín

<sup>1</sup>*Department of Mechanical, Energetic and Materials Engineering. School of Industrial Engineering.  
University of Extremadura. Elvas Avenue s/n, 06006, Badajoz. Spain*

<sup>2</sup>*Department of Graphic Expression. School of Industrial Engineering. University of Extremadura.  
Elvas Avenue s/n, 06006, Badajoz. Spain*

<sup>3</sup>*Department of Materials Science and Metallurgical Engineering. Chemical Sciences Faculty.  
Complutense University of Madrid. Complutense Avenue s/n, 28040, Madrid. Spain*

## Abstract

Activated carbons were prepared from kenaf by chemical activation with phosphoric acid in different concentrations. Its electrical conductivity was also determined. From the series of prepared activated carbons, those with better textural properties, chemistry and high electrical conductivity were selected for their use in adsorption and electroadsorption processes.

The removal of Cu (II) ions from aqueous media is of great interest due to their harmful effects on health and environment. The aim of this work was to study the kinetics in the process of retention of copper ions in aqueous solution by adsorption and electroadsorption using activated carbon. Thus, when comparing both processes it was observed that the adsorption equilibrium times were generally greater than those corresponding to electroadsorption. Different kinetic models were applied. The kinetic models applied to the adsorption/electroadsorption processes indicated that the pseudo-second order model described both processes in a better way than the pseudo-first order model. The values of R<sup>2</sup> in electroadsorption kinetics were closer to 1 than those obtained in adsorption kinetics. Therefore, it can be affirmed that the pseudo-second order model for the samples, object of study, is better adjusted to the electroadsorption process.

**Keywords:** Activated carbon; Adsorption; Electroadsorption; Kinetics model; Copper ion.

\*Corresponding author:

E-mail address: [amacgar@unex.es](mailto:amacgar@unex.es) (A. Macías-García)

## 1. Introduction

Activated carbons (ACs) have a crystalline structure of graphitic type that is characterized by high volume of micropores and mesopores, which gives the material a high surface area. However, commercial AC can be regarded as relatively expensive for some applications. Consequently, the use of agricultural biomass waste as a precursor to the manufacture of AC [1–3] emerges as an alternative.

Kenaf is an appropriate material for being used as precursor in the manufacture of AC.

It is a dicotyledonous plant, belonging to the genus *Hibiscus* (Malvaceae family). Kenaf is a good source of biomass due to its abundance, since it can grow under a wide range of climatic conditions requiring minimal amounts of water, fertilizers or pesticides. It is also a plant rich in cellulose. The stem of the kenaf plants consists of an outer bark and an inner core, both containing fibrous components that can be used for adsorption [4-5].

In the activation process to obtain an activated carbon, it is necessary to take into account the type of precursor and the activation agents, since the use of different compounds provides an AC with several porous properties and structures [6]. The  $\text{H}_3\text{PO}_4$  is an activating agent that allows to work at low temperatures (over 400 °C). Furthermore, it does not cause corrosion in the equipment and leaves no metallic residues, which makes it respectful of the environment, and provides AC micro- and mesopores with high surface area [5],[7-8].

Materials with the properties above described are suitable for adsorption of harmful substances to humans and environment [9-10]. Clear examples of these harmful substances are heavy metals that are found in our environment above controlled levels. The term heavy metals is applied to those elements whose atomic weight is between 63.5 and 200.6, and have a specific gravity above 5.0 [3]. These materials are non-biodegradable and have a tendency to be accumulated in living organisms. This is why

the level of these heavy metals in the environment is increasing day by day. The main sources of these heavy metals are wastewater pollution in industrial processes, metal cleaning, boiler piping, and fertilizer production.

Copper is a heavy metal that is particularly harmful to humans, a long exposure to copper above acceptable concentration levels can result in irritation of nose, mouth and eyes, headaches, nausea, vomiting, diarrhoea and, in extreme cases, can damage the kidneys for life and cause death [9],[11–13].

Electroadsorption is defined as an adsorption phenomenon induced by a potential difference applied on the surface of an electrode [14]. When an external electric field is imposed between two electrodes immersed in an electrolytic solution, the ions are forced to move towards the opposite charge electrodes, this resulting in a separation of charges through the electrode/dissolution interface [15]. This phenomenon can significantly improve the adsorption capacity of activated carbons without the need of impregnation. This is due to the fact that the electronic density of the adsorbent changes with the potential applied, this favouring the interaction with the ionic species in the dissolution [16].

In this work, the study of  $\text{Cu}^{2+}$  ion adsorption/electroadsorption and its kinetic model was performed using activated carbon. Activated carbons were obtained from kenaf and activated by  $\text{H}_3\text{PO}_4$ .

## **2. Experimental.**

The materials used have been:

- Kenaf (K), from which activated carbon (AC) has been prepared by chemical activation.
- Carbon black Vulcan 3 (V3), from Cabot Corporation, used to improve the electrical conductivity of the prepared samples.

- Polyvinylidene fluoride (PVDF), powder, provided by Aldrich (Sigma-Aldrich Chem., S.L.) and used in this work as binder for the preparation of activated carbon electrodes.

25 g of kenaf were impregnated with 100 ml  $\text{H}_3\text{PO}_4$  (at concentrations of 36%, 60%, and 85%) at 85 °C during 2h. The solid product was subjected to a heat treatment at different temperatures 350-550 °C, with a heating rate of 5 °C  $\text{min}^{-1}$  in a  $\text{N}_2$  atmosphere (rate flow of 85  $\text{ml}\cdot\text{min}^{-1}$ ). Isothermal conditions at the selected temperature were maintained during 2 h. Finally, the product was washed using distilled water (neutral pH) and dried at 120 °C. The phosphoric acid used and existing in the washing water is recovered and reused.

The chemical characterization was carried out using two tests: chemical analysis, and surface functional groups analysis. The textural characterization of the samples was performed by nitrogen adsorption and mercury porosimetry. The DC electrical conductivity (S) was measured at room temperature by impedance spectroscopy over the frequency range from 20 to  $10^6$  Hz at a voltage of 1V.

The kinetic study of the adsorption process was carried out. For measuring an adapter was designed in three dimensions to be incorporated into a thermostatic bath with agitation (Figure 1). This adapter supported vessels containing carbon samples in contact with Cu (II) ion dissolution. The adapter designed in 3D allows the recipients to be subjected to pressure in each hole and, as a result, to the same agitation speed.



**Figure 1. Adapter designed in 3D to be incorporated into a thermostatic bath.**

The electrodes to be studied were prepared from various raw materials. These raw materials were Carbon Black (Vulcan 3, V3), Polyvinylidene fluoride (PVDF, supplied by Sigma-Aldrich Chemical S.L.), and activated carbons P-60-450, P-60-500 and P-60-550.

The kinetic study of the electroadsorption process was performed in a system of integrated electrodes (designed in 3D) to support cylindrical activated carbon electrodes (Figure 2). This support allows the contact between the cylindrical carbon electrodes and the dissolution of Cu (II) ions.

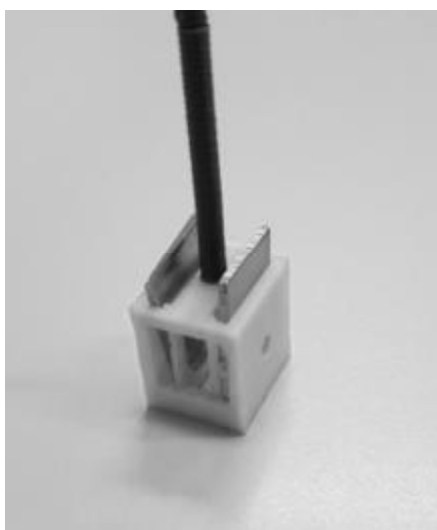


**Figure 2. System of integrated electrodes (designed in 3D).**

The advantage of this design (Figure 2) is that it allows, on the one hand, maintaining the parallelism of the electrodes, which facilitates the process of electroadsorption ,and

on the other hand, modifying the distance of separation between the electrodes until reaching the optimal distance.

In order to study the adsorption/electroadsorption kinetics, fixed amounts of adsorbent 0.1g of activated carbon and volumes of adsorptive solution(80 mL) of a given initial concentration  $25 \text{ mg}\cdot\text{L}^{-1}$  of  $\text{CuSO}_4$  were kept in contact at constant temperature for a given period of time previously set. With the aim of checking the evolution of the adsorption process with time, the concentration of solute was analysed. The equilibrium time,  $t_e$ , may be defined as the minimum period of time that is necessary to keep the value of concentration unvaried.

The Cu (II) ion concentration was measured with the aid of a Perkin Elmer flame atomic absorption spectrometer (Model Thermo Corporation). In this study, different kinetic models were tested: pseudo-first order model, pseudo-second order model, and intraparticle diffusion.

### 3. Results and Discussion

The interest in the application of carbons as electrodes has increased in recent years [17]. This interest is due to the properties of carbonaceous materials, such as electrical conductivity, specific surface, pore distribution, and easy processibility.

In view of the results previously obtained, it is of great importance to study the behaviour of the samples prepared in the process of adsorption/electroadsorption.

#### 3.1. Textural characterization

**Table 1. Textural parameters of ACs prepared with  $\text{H}_3\text{PO}_4$ .**

Sample	$S_{\text{BET}}$ ( $\text{m}^2\cdot\text{g}^{-1}$ )	$V_{\text{mi}}$ ( $\text{cm}^3\cdot\text{g}^{-1}$ )	$V_{\text{me}}$ ( $\text{cm}^3\cdot\text{g}^{-1}$ )	$V_{\text{me-p}}$ ( $\text{cm}^3\cdot\text{g}^{-1}$ )	$V_{\text{ma-p}}$ ( $\text{cm}^3\cdot\text{g}^{-1}$ )
P- 36- 350	600	0.33	0.11	0.11	0.16
P- 36- 400	799	0.48	0.14	0.14	0.21
P- 36- 450	955	0.54	0.21	0.21	0.22
P- 36- 500	1556	0.88	0.22	0.22	0.25
P- 36- 550	1804	1.02	0.33	0.33	0.25
P- 60- 350	853	0.40	0.17	0.25	0.28
P- 60- 400	1255	0.50	0.40	0.29	0.34
P- 60- 450	1567	0.62	0.65	0.35	0.34

P-60-500	2270	0.88	1.15	0.35	0.42
P-60-550	2145	0.98	0.63	0.40	0.43
P- 85- 350	955	0.54	0.67	0.63	0.32
P-85-400	1208	0.68	0.76	0.60	0.44
P- 85- 450	1496	0.84	0.86	0.86	0.54
P- 85- 500	1957	1.11	0.96	0.96	0.59
P- 85- 550	1934	1.10	1.04	1.04	0.64

Table 1 shows the values of the textural parameters for the three series of ACs. These values were obtained from the adsorption isotherms of N<sub>2</sub> at -196 °C and the curves of the accumulated pore volume versus the pore radius (mercury porosimetry). The highest values of surface area and pore volume correspond to the samples of ACs prepared using phosphoric acid solutions with the higher concentrations (60 or 85%) and heating to the two highest temperatures (500 or 550 °C).

The development of porosity, that results from the carbonisation of the starting material above a certain temperature (>450 °C) through activation with H<sub>3</sub>PO<sub>4</sub>, is related to the fact that the phosphorus species present in the impregnated product tend to pass into the gas phase, this causing a structural expansion in the product [18]. According to Jaytoyen and Derbyshire [19], the development of porosity below 450 °C is related to the stabilization and expansion of lignocellulosic material structure. Cross-linking reactions begin to dominate over bonds rupture and depolymerisation reactions. These researchers proposed that the formation and stability of the phosphocarbonaceous esters at this temperature limit depolymerisation and consequently the development of porosity.

### **3.2. Chemical characterization**

Regarding the analysis of surface functional groups, the FT-IR spectra obtained for P-60-T series samples showed three very wide bands with maximum absorption peaks located at 3400, 1600 and 1200 cm<sup>-1</sup>.

At 3400 cm<sup>-1</sup> the band associated with O-H stretching vibrations in alcohols and

carboxylic acids is located. It should be noted that the intensity of this band in the samples is proportional to the concentration of acid groups found for each of them.

The energy absorption in these areas of the infrared spectrum is attributable to the tension vibrations of the O-H, C=C and =CH bonds. The band at  $1600\text{ cm}^{-1}$  is due to the presence of C=C groups corresponding to aromatic rings. In the spectrum region around  $1200\text{ cm}^{-1}$ , a vibration band is observed in the plane =CH of the aromatics =CH [20]. On the other hand, due to the tension vibration of the P-O and P=O bonds, spectral bands were registered at  $1260\text{--}855\text{ cm}^{-1}$  and  $1300\text{--}960\text{ cm}^{-1}$ , respectively. For P-C bond, however, the band was located between  $800\text{--}900\text{ cm}^{-1}$  [21]. Finally, the peak at  $1710\text{ cm}^{-1}$  was easily visible in the spectra of these series (see Figure 3).

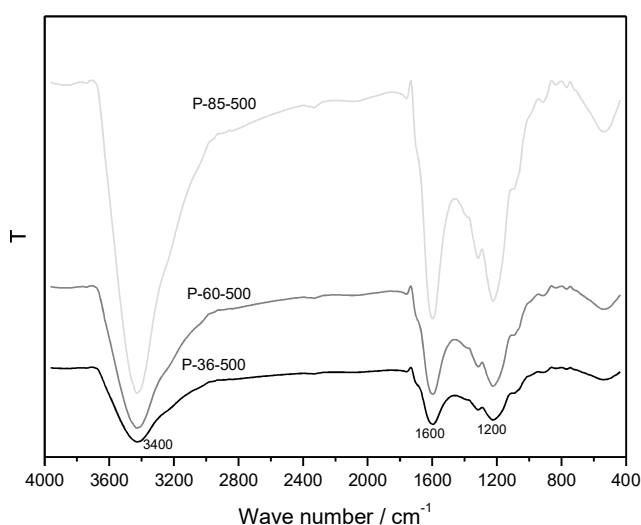


**Figure 3. FT-IR spectra for P-T-500 series**

### 3.3. Electrical conductivity

In recent years the application of carbons as electrodes [22-23] has grown due to their electrical conductivity, specific surface, pore distribution, surface chemical composition and easy processibility.

In view of the results obtained, carbons with the largest specific surface area and

porosity distribution, series P-60-T, were the object of study in terms of electrical conductivity. According to the bibliography consulted, this type of carbon can be good precursors for being used as supercapacitors [10],[24],[25],[26].

Figure 4 shows the variation of the electrical conductivity of the samples (P-60-T series) with pressure during the compaction process.

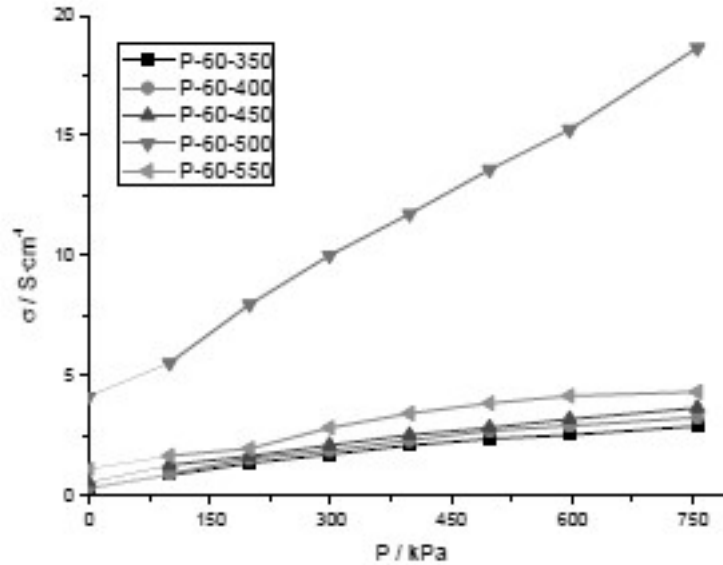


**Figure 4 Variation of the electrical conductivity with pressure (P-60-T series).**

Figure 4 shows that, during the activation process of the carbon, aromatic structures can be formed, which may favour an increase in conductivity. The increased electrical conductivity of the P-60-500 sample may be due to the existence of graphical structures, aromatic rings, oxygen groups, etc., which allows a higher level of mobility to be produced in the electrons or, in other words: a much higher degree of electricity transfer is produced.

Activated carbon is a carbonaceous material that has a crystalline structure similar to that of graphite except that the order in the structure of activated carbon is less perfect. That is to say, the difference between activated carbon and graphite consists in the degree of arrangement in the three coordinates of the space presented by graphite, whereas in the CA there are only two, which correspond to the independent planes constituted by the plates that they conform it, these plates have different orientations.

199 Chemical activation does not produce the same graphite plates that result from the  
200 physical activation method. The walls of the carbon rather resemble an organic  
201 molecule, part aromatic and part aliphatic, or a polymer highly branched and  
202 interlinked, furthermore these walls contain large quantities of atoms other than carbon,  
203 mainly oxygen. This fact is verified in the FT-IR spectra where the presence of aromatic  
204 structures is evident.

205 Among other reasons, this behaviour may be due to the fact that this carbon forms  
206 layers of carbon rings linked together. These rings contain single and double bonds, this  
207 giving rise to delocalized electrons by the double bonds of each carbon (pi bonds).  
208 These delocalized electrons move from one side to another generating a current when a  
209 potential is applied. This phenomenon only takes place if the potential difference goes  
210 parallel to the carbon layer. This process does not occur in carbon structures where each  
211 carbon is linked to four more carbon through very resistant simple bonds with a null  
212 electron delocalization, this being the reason by which they are “tied” to that bond.

213 The behaviour of P-60-550 sample could be due to pulverized activated carbon, which  
214 can lead to repulsion problems between its particles and/or decreases in electrical  
215 conductivity, as described by various authors in carbon blacks [6].

216 It was observed that when increasing the pressure, the conductivity increased in all  
217 samples (see Figure 4). This behaviour is probably due to the loss of porosity and the  
218 greater number of contacts between AC particles.

219 If we look at the values obtained for the P-60-T series samples, we can affirm that P-  
220 60-450, P-60-500, and P-60-550 samples would be the most suitable to be tested as  
221 possible supercapacitors.

### ***3.4. Adsorption and electroadsorption of samples prepared by chemical activation with $H_3PO_4$ .***

Adsorption consists of the migration of some substances from the gaseous or liquid phase to the surface of a solid substrate. ElectroadSORPTION is generally defined as an adsorption phenomenon induced by a potential difference on the surface of an electrode [27].

In these adsorption/electroadSORPTION processes, the adsorption/electroadSORPTION velocity will depend fundamentally on the nature of the adsorbent, but also on other factors. In recent years, many researches have been done to understand the behaviour of activated carbon electrodes in electroadsorption processes. It has been shown that the shape, size and pore volume, and pore size distribution have a great influence on the kinetics of electroadsorption [28], [29]. On the other hand, the presence of heteroatoms (such as nitrogen atoms) and/or surface groups in the structure of the activated carbon electrodes can also have a great influence on the electroadsorption processes [28].

In the following section, the results obtained in the kinetics of the adsorption and electroadsorption process are discussed.

#### ***3.4.1 Kinetic study***

The kinetic study allows determining the rate of adsorbate adsorption and provides an idea of the adsorption mechanism. According to Adamson [30], the step that leads to the link between adsorbate and adsorbent is very fast when taking place a physical adsorption, where the adsorption rate is controlled by the previous diffusion. If adsorption is accompanied by a chemical reaction, adsorption is slow because the chemical reaction is slower than the diffusion step.

Kinetic adsorption/electroadSORPTION models are important in studies carried out on the

retention of heavy metal ions in wastewater. In this work, various kinetic models above described were tested. The velocity constants of each kinetic equation and the adsorption/electroadsorption parameters were calculated.

The concentration/time kinetic curves are shown in Fig. 5. According to Figure 5, a rapid adsorption/electroadsorption took place within the first few minutes. After this initial times the adsorption/electroadsorption gradually decreased, the equilibrium being reached at different contact times depending on the carbonaceous sample.

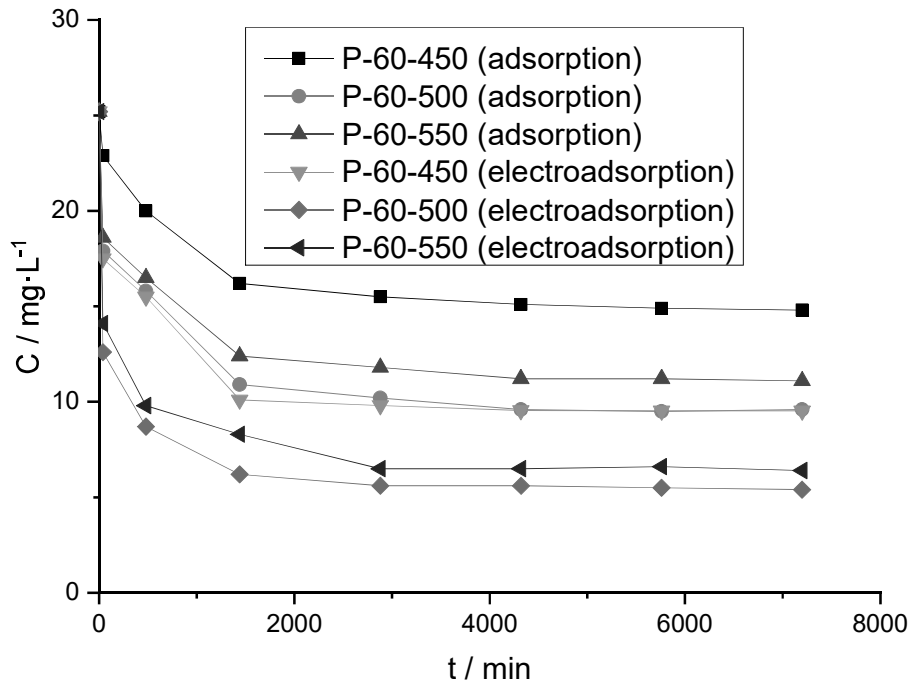


**Figure 5. Adsorption and electroadsorption kinetics of the prepared samples.**

By comparing the kinetics curves of adsorption and electroadsorption, it is observed that the adsorption process takes place fundamentally in the first 4320 minutes, while the electroadsorption process is produced within the first 2880 minutes. Subsequently, it does not significantly increase the amount adsorbed, the equilibrium being reached.

**Table 2. Equilibrium times and retained quantities of Cu (II) ions in the kinetic process of adsorption and electroadsorption. Samples activated with H<sub>3</sub>PO<sub>4</sub>.**

Samples	t <sub>e</sub> (adsorption) min	q <sub>e</sub> mg·g <sup>-1</sup>	t <sub>e</sub> (electroadsorption) min	q <sub>e</sub> mg·g <sup>-1</sup>
P-60-450	5760	8.3	4320	12.5
P-60-500	4320	1.5	2880	15.8
P-60-550	4320	1.3	2880	15.0

Likewise, when comparing both processes it is observed that the adsorption equilibrium times are generally greater than those corresponding to electroadsorption (see Table 2). This significant difference in equilibrium times can be explained taking into account that adsorption involves the transfer of a substance from the dissolution to the adsorbent surface. However in electroadsorption, the adsorption process must be supplemented by the action of an external electric field between two electrodes immersed in an electrolytic solution. This electric field causes the charged ions to be forced to move towards the opposing charge electrodes, this giving rise to a charge separation throughout the electrode/dissolution interface [15-16].

Both in adsorption and electroadsorption process, the same sequence of adsorption capacity of the samples was observed, this being P-60-500 > P-60-550 > P-60-450. This fact could be related, on the one hand, to the presence of superficial groups, and, on the other hand, to the distribution of porosity in the samples. In particular, it could be related to the mesopores, which would facilitate the diffusion of adsorbate into the activated carbon, as observed in sample P-60-500 and gathered in Table 1 ( $V_{me, narrow} = 1.15 \text{ cm}^3 \cdot \text{g}^{-1}$ , and  $V_{me, wide} = 0.35 \text{ cm}^3 \cdot \text{g}^{-1}$ ).

#### *3.4.1.1. Kinetic models of the processes*

The design and study of an adsorption system requires knowledge of the equilibrium and kinetics of adsorption. The kinetics of a chemical process depends on material factors (adsorbents and adsorbates used) such as experimental factors (temperature and pH) [31-32]. The two most used kinetic models in the study of the adsorption process in liquids are pseudo-first-order and pseudo-second-order. Numerous studies have attempted to rationalize these two empirical models [33-36] and review their applications to different chemical systems [37-39].

On the other hand, the theoretical complexity of adsorption mechanisms has developed different kinetic models to predict the amount of adsorbate adsorbed on the adsorbent [37], [40-41].

Considering the complexities and restriction of the theoretical models, the empirical or at best 'rationalized' empirical models, such as the pseudo-order models, shall remain relevant and attractive in the modelling of liquid adsorption kinetics for practical purposes.

#### *3.4.1.1.1 Pseudo-first order model*

The pseudo-first order kinetics are based on the hypothesis that each metallic ion is assigned an adsorption site of the adsorbent material.

To check whether the adsorption/electroabsorption process of copper ions on activated carbon complies with the mathematical expression applicable to the first order kinetics, a linear adjustment of the experimental data was performed.

Graphs of  $\log(q_e - q_t)$  versus time of the adsorption process are shown in Figure 6. The values of  $k_1$  and the correlation coefficient,  $R^2$ , for all samples are gathered in Table 3.  $R^2$  values varied from 0.9028 to 0.9684 for the adsorption process (see Table 3-A), and from 0.7219 to 0.9521 for the electroadsorption process (see Table 3-B). Likewise, a bad correlation was observed between the values of experimental  $q_e$  (see Table 2) and

those obtained by the pseudo-first order model (see Table 3)

Therefore, we can conclude that neither of the two processes fits well with the pseudo-first order model. However, the Cu (II) ion adsorption fits better than its electroadsorption.

**Table 3. Kinetic parameters of adsorption (A) and electroadsorption (B).**

**(A) Adsorption**

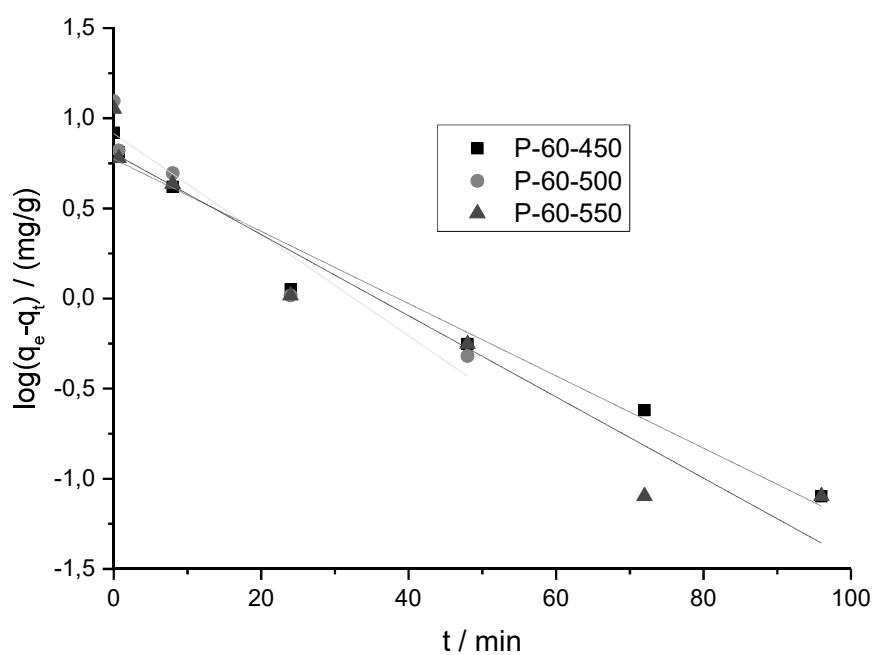
Samples	Pseudo-primer order			Pseudo-second order		
	$q_e$	$k_1$	R	$q_e$	$k_2$	R
P-60-450	5.9	$7.7 \cdot 10^{-4}$	0.9684	8.7	$3.5 \cdot 10^{-4}$	0.9981
P-60-500	8.2	$1.1 \cdot 10^{-3}$	0.9028	1.8	$4.3 \cdot 10^{-4}$	0.9986
P-60-550	6.4	$8.6 \cdot 10^{-4}$	0.9295	1.6	$4.6 \cdot 10^{-4}$	0.9990

Samples	Diffusion		
	C	$k_{id}$	R
P-60-450	3.2	$1.6 \cdot 10^{-1}$	0.9970
P-60-500	2.5	$2.3 \cdot 10^{-1}$	0.9993
P-60-550	0.9	$1.3 \cdot 10^{-1}$	0.9958

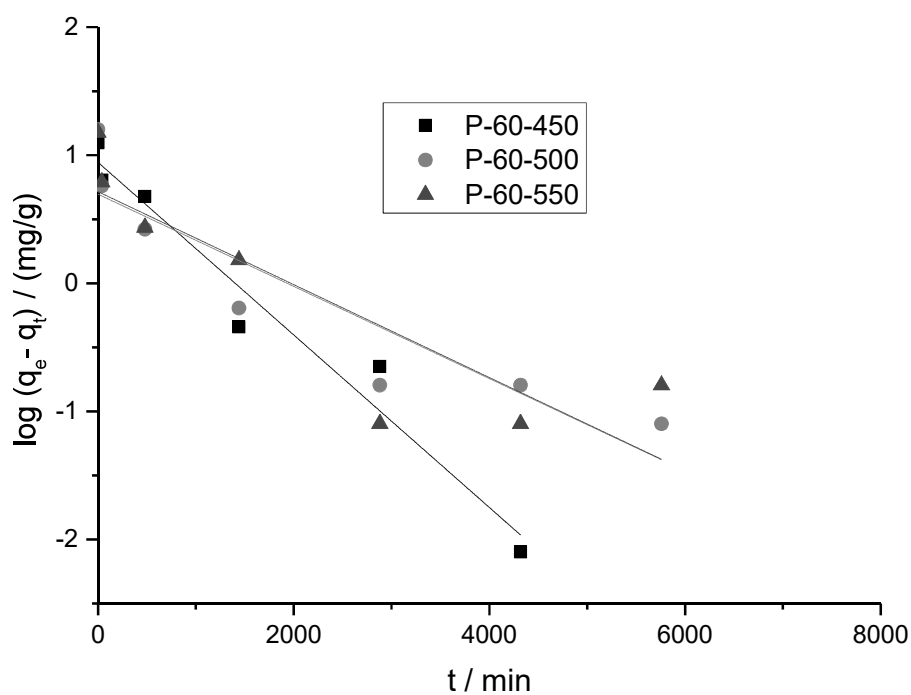
**(B) Electrodesorption**

Samples	Pseudo-primer order			Pseudo-second order		
	$q_e$	$k_1$	R	$q_e$	$k_2$	R
P-60-450	8.8	$1.6 \cdot 10^{-3}$	0.9521	12.8	$5.6 \cdot 10^{-4}$	0.9988
P-60-500	5.0	$8.4 \cdot 10^{-4}$	0.8205	15.9	$1.0 \cdot 10^{-3}$	0.9999
P-60-550	5.2	$8.4 \cdot 10^{-4}$	0.7219	15.2	$7.3 \cdot 10^{-4}$	0.9996

Samples	Diffusion		
	C	$k_{id}$	R
P-60-450	4.5	$1.9 \cdot 10^{-1}$	0.8918
P-60-500	9.6	$2.6 \cdot 10^{-1}$	0.9507
P-60-550	8.3	$1.5 \cdot 10^{-1}$	0.9835



(A)



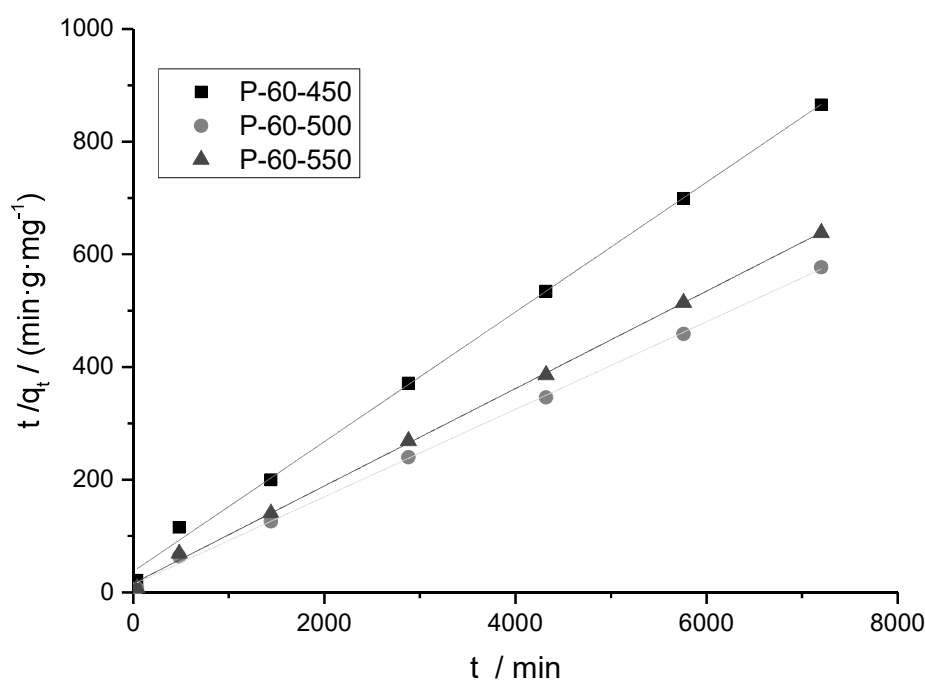
(B)

**Figure 6. Graphic representation of the pseudo-first order model: (A) adsorption, (B) electroadsorption.**

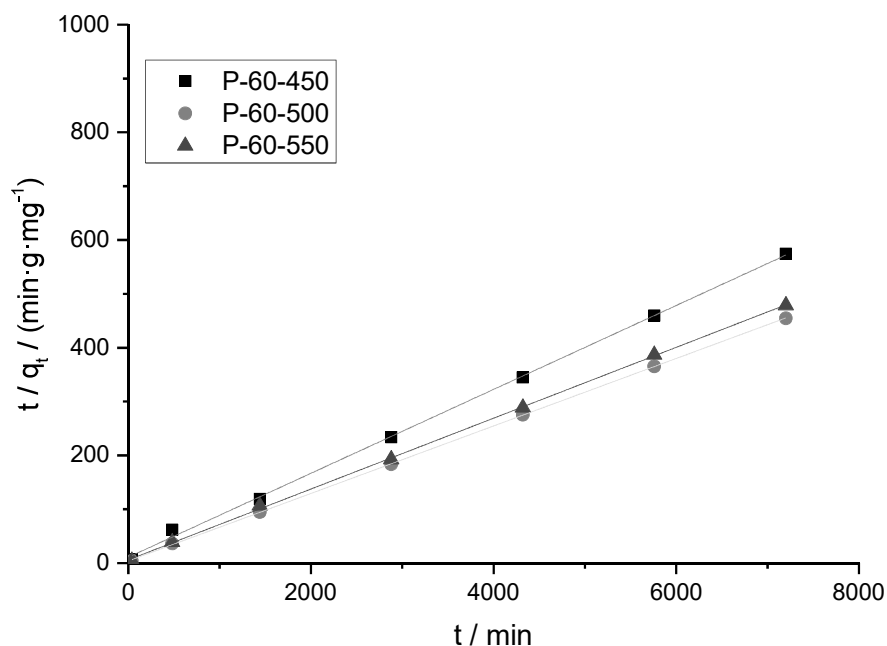
### 3.4.1.1.2 Pseudo-second order model

The experimental data were adjusted to the pseudo-second order kinetic model. Figure 3.5 shows the graphs that represents  $t/q_t$  versus time. From the slope the  $q_e$  value was obtained, while the intercept provided the  $k_2$  value.

The kinetic parameters obtained in the adsorption/electroadsorption process are gathered in Table 3. This model fits better than the pseudo-first order model according to the values of the correlation coefficients  $R^2$ , which are closer to the unit. This indicates that copper is chemisorbed on the surface of the activated carbon. Similar behaviour was reported by other authors for this type of adsorption kinetic model applied to other metals [42-47].



(A)



(B)

**Figure 7. Graphic representation of pseudo-second order model: (A) adsorption; (B) electroadsorption**

Figure 7 shows how the kinetic model of pseudo-second order suitably describes the adsorption of copper in the activated carbon samples prepared in this series. Moreover, and as gathered in Table 3, the correlation coefficients were generally higher than 0.9981 and were over the obtained with the pseudo-first order model. This suitable behaviour could be explained by the adsorption/electroadsorption mechanism in the process, which involves the valence forces through the sharing or exchange of electrons between the copper ions and the adsorbent. In addition, the adsorption capacity of activated carbons is directly proportional to the active sites occupied by copper ions, which means that adsorbate is adsorbed in two active sites of activated carbons.

Table 3 shows that the values of  $R^2$  are closer to 1 in electroadsorption kinetics than in adsorption kinetics. Therefore, it can be affirmed that the pseudo-second order model

is better adjusted to the electroadsorption process of the samples under study.

In the particular case of adsorption, and as gathered in Table 3, it was observed that the P-60-450 sample had lower kinetic parameters than the P-60-500 and P-60-550 samples. This indicates, on the one hand, that kinetics are slower ( $k_2$  lower), and, on the other hand, that the concentration in the equilibrium  $q_e$  ( $8.3 \text{ mg}\cdot\text{g}^{-1}$ ) is similar to the  $q_e$  calculated by the kinetic model ( $8.7 \text{ mg}\cdot\text{g}^{-1}$ ). Kinetic behaviour is similar for the samples P-60-500 and P-60-550, as reflected in the kinetic parameters gathered in Table 3.3. This could be related to the similar porous texture (see Table 1) and the presence of oxygenated groups in both samples (see Figure 3).

On the other hand, in the electroadsorption process (see Table 3.B), it is observed that the  $k_2$  value of the P-60-500 sample is greater than those corresponding to the other samples, which indicates that its kinetics is faster. This faster kinetic could be related not only to the presence of superficial groups, but also to the presence of mesoporous structures previously mentioned. Also, the correlation between the experimental  $q_e$  values (see Table 2) and the calculated  $q_e$  values (see Table 3) through the pseudo-second order kinetic model was very good.

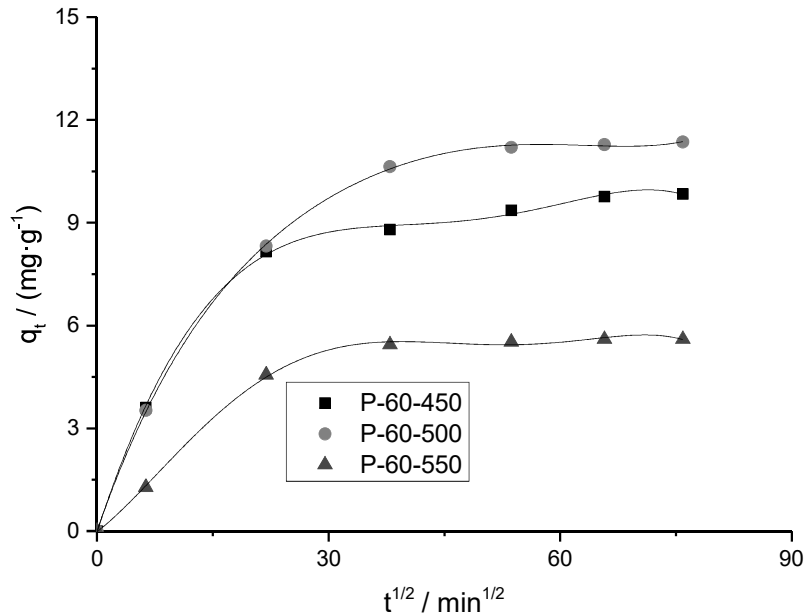
According to the obtained results, it can be concluded that both processes are well adjusted to the kinetic model of pseudo-second order, especially for electroadsorption process.

#### *3.4.1.1.3. Intraparticle diffusion*

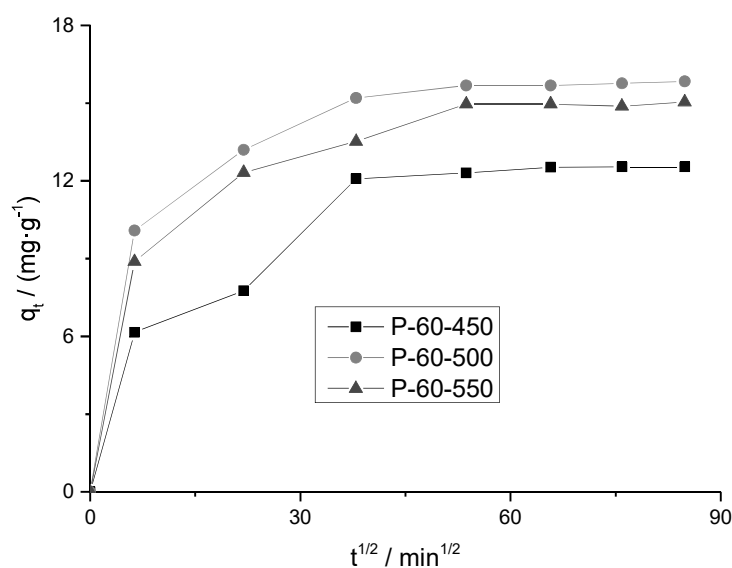
The Weber and Morris intraparticle diffusion model was also used to describe the kinetics of Cu (II) absorption. This model assumes that if the regression of  $q_t$  vs.  $t^{1/2}$  is linear and passes through the origin, intraparticle diffusion is the only rate-limiting step[48-50]. However, this is not always the case, since other processes, such as surface diffusion and equilibrium adsorption, may also limit the velocity at different stages of

the kinetic profile, which would result in a multi-linearity in the intraparticle diffusion plot [51].

Plots of  $q_t$  versus  $t^{1/2}$  for the adsorption (see Figure 8-A) and electroadsorption process (see Figure 8-B) show two linear sections. The slope of the first section, approximately between 6 and 40  $\text{min}^{1/2}$ , corresponds to the two adsorption/electroadsorption processes and is more pronounced than the slope of the second section. This difference shows that the diffusion process is faster in this first section. This fact would be associated with the diffusion of adsorbate through the liquid-solid interface, the linear behaviour indicating a quickly mass transport. The second linear section corresponds to values of  $t^{1/2}$  between 53 and 87  $\text{min}^{1/2}$  and is associated with the transport of adsorbate into the adsorbent pores (internal diffusion). This behaviour seems to also indicate that this stage takes place quickly. However, from samples shown in Figure 8, it is deduced that the values of the correlation coefficients are quite different from the unit (see Table 3).



(A)



(B)

**Figure 8. Graphic representation of the intraparticle diffusion model: (A) adsorption; (B) electroadsorption.**

In general, it is observed that mass diffusion values, from the surface to the interior of activated carbon ( $k_{\text{dif}}$ ), and the boundary of the mass transfer layer (C) are increased in the electroadsorption process (see Table 3). Higher values of C indicate a greater surface participation in metal adsorption. For P-60-500 and P-60-550 samples, which have the best electroadsorption capacity, the highest values of  $q_t$  can be observed, while P-60-500 sample has the best adsorption capacity.

#### 4. Conclusions

The preparation, characterization and use of activated carbons was carried out in this study. Prepared samples showed a high specific surface area and notable porous development.

The increase of the concentration of the solution of phosphoric acid, activant agent, develops in the samples a greater superficial area and an increase in the volume of micropore; furthermore it has an influence on the superficial chemistry of the

carbonaceous material, presenting variations in the quantity of acid groups, which were characterized by infrared spectroscopy.

From textural parameters, chemical analysis and electrical conductivity, the three best activated carbons were selected for their application in the adsorption/electroadsorption process, these being P-60-450, P-60-500, and P-60-550.

The equilibrium time in the electroadsorption process was lower than the equilibrium time in the adsorption process. The pseudo-second order model fitted better than the pseudo-first order model, since the values of the correlation coefficients  $R^2$  were closer to the unit. This indicates that copper is chemisorbed on the surface of the activated carbon.

Intraparticle diffusion plots have two stages. The first stage is due to an instantaneous adsorption or adsorption on the outer surface, where the adsorbate travels to the outer surface of the adsorbent. In the second stage a gradual adsorption occurs where the intraparticle diffusion is the velocity limiting, i.e., the adsorbate travels within the pores of the adsorbent.

Thus, according to the results obtained, the sample with the highest copper retention capacity was sample P-60-500. The greater elimination capacity of the Cu (II) ions evidenced by the sample P-60-500, due to its harmful effects on health and the environment, is undoubtedly a result of great interest.

## 5. References

- [1] C. Santhosh, V. Velmurugan, G. Jacob, S. K. Jeong, A. N. Grace, and A. Bhatnagar, "Role of nanomaterials in water treatment applications: A review," *Chem. Eng. J.*, vol. 306, pp. 1116–1137, 2016.
- [2] G. A. Adebisi, Z. Z. Chowdhury, and P. A. Alaba, "Equilibrium, kinetic, and thermodynamic studies of lead ion and zinc ion adsorption from aqueous solution onto activated carbon prepared from palm oil mill effluent," *J. Clean. Prod.*, vol.

148, pp. 958–968, 2017.

- [3] N. P. Raval, P. U. Shah, and N. K. Shah, “Adsorptive removal of nickel(II) ions from aqueous environment: A review,” *J. Environ. Manage.*, vol. 179, pp. 1–20, 2016.
- [4] M. Ramesh, “Kenaf (*Hibiscus cannabinus* L.) fibre based bio-materials: A review on processing and properties,” *Prog. Mater. Sci.*, vol. 78–79, pp. 1–92, 2016.
- [5] M. S. Shamsuddin, N. R. N. Yusoff, and M. A. Sulaiman, “Synthesis and Characterization of Activated Carbon Produced from Kenaf Core Fiber Using  $H_3PO_4$  Activation,” *Procedia Chem.*, vol. 19, pp. 558–565, 2016.
- [6] E. M. Cuerda-Correa, A. Macías-García, M. A. D. Díez, and A. L. Ortiz, “Textural and morphological study of activated carbon fibers prepared from kenaf,” *Microporous Mesoporous Mater.*, vol. 111, no. 1–3, pp. 523–529, 2008.
- [7] Y. Sun, H. Li, G. Li, B. Gao, Q. Yue, and X. Li, “Characterization and ciprofloxacin adsorption properties of activated carbons prepared from biomass wastes by  $H_3PO_4$  activation,” *Bioresour. Technol.*, vol. 217, pp. 239–244, 2016.
- [8] B. Meryemoglu, S. Irmak, and A. Hasanoglu, “Production of activated carbon materials from kenaf biomass to be used as catalyst support in aqueous-phase reforming process,” *Fuel Process. Technol.*, vol. 151, pp. 59–63, 2016.
- [9] M. Bilal *et al.*, “Waste biomass adsorbents for copper removal from industrial wastewater-A review,” *J. Hazard. Mater.*, vol. 263, pp. 322–333, 2013.
- [10] D. Kołodyńska, J. Krukowska, and P. Thomas, “Comparison of sorption and desorption studies of heavy metal ions from biochar and commercial active carbon,” *Chem. Eng. J.*, vol. 307, pp. 353–363, 2017.
- [11] A. Macías-García, M. Gómez Corzo, M. Alfaro Domínguez, M. Alexandre Franco, and J. Martínez Naharro, “Study of the adsorption and electroadsorption process of Cu (II) ions within thermally and chemically modified activated carbon,” *J. Hazard. Mater.*, vol. 328, pp. 46–55, 2017.
- [12] Z. Z. Chowdhury, S. M. Zain, R. A. Khan, and M. S. Islam, “Preparation and characterizations of activated carbon from kenaf fiber for equilibrium adsorption studies of copper from wastewater,” *Korean J. Chem. Eng.*, vol. 29, no. 9, pp. 1187–1195, 2012.
- [13] C. M. Hasfalina, R. Z. Maryam, C. A. Luqman, and M. Rashid, “Adsorption of Copper (II) From Aqueous Medium In Fixed-Bed Column By Kenaf Fibres,” *APCBEE Procedia*, vol. 3, no. May, pp. 255–263, 2012.

- 480 [14] Y. Han, X. Quan, S. Chen, H. Zhao, C. Cui, and Y. Zhao, "Electrochemically  
481 enhanced adsorption of phenol on activated carbon fibers in basic aqueous  
482 solution," *J. Colloid Interface Sci.*, vol. 299, no. 2, pp. 766–771, 2006.
- 483 [15] H. Li, Y. Gao, L. Pan, Y. Zhang, Y. Chen, and Z. Sun, "Electrosorptive  
484 desalination by carbon nanotubes and nanofibres electrodes and ion-exchange  
485 membranes," *Water Res.*, vol. 42, no. 20, pp. 4923–4928, 2008.
- 486 [16] E. J. Bain, J. M. Calo, R. Spitzsteinberg, J. Kirchner, and J. Ax, "Electrosorption  
487 / Electrodesorption of Arsenic on a Granular Activated Carbon in the Presence of  
488 Other Heavy Metals <sup>†</sup>," *Energy Fuels*, pp. 3415–3421, 2010.
- 489 [17] M. E. Ramos, P. R. Bonelli, and A. L. Cukierman, "Physico-chemical and  
490 electrical properties of activated carbon cloths. Effect of inherent nature of the  
491 fabric precursor," *Colloids Surfaces A Physicochem. Eng. Asp.*, vol. 324, no. 1–3,  
492 pp. 86–92, 2008.
- 493 [18] M. Olivares-Marín, C. Fernández-González, A. Macías-García, and V. Gómez-  
494 Serrano, "Porous structure of activated carbon prepared from cherry stones by  
495 chemical activation with phosphoric acid," *Energy and Fuels*, vol. 21, no. 5, pp.  
496 2942–2949, 2007.
- 497 [19] M. Jagtoyen and F. Derbyshire, "Activated carbons from yellow poplar and white  
498 oak by H3PO4 activation," *Carbon N. Y.*, vol. 36, no. 7–8, pp. 1085–1097, 1998.
- 499 [20] J. Karen, H. Peña, Liliana Giraldo, Juan Carlos Moreno. Preparation of activated  
500 carbon from orange peel by chemical activation. Physical and chemical  
501 characterization. *Rev. Colomb. Quím.*, 41(2): 311–323, 2012
- 502 [21] W. Pretsch, E. Clerc, T. Seibl, J. Simon, "Tables of Spectral Data for Structure  
503 Determination of Organic Compounds". Translation by K. Biemann.  
504 Springer- Verlag, Berlin, Heidelberg, New York, Tokyo, 1983. 316 pp.
- 505 [22] E. Frackowiak and F. Beguin, "Carbon Materials for the Electrochemical Storage  
506 of Energy in capacitors," *Carbon N. Y.*, vol. 39, pp. 937–950, 2001.
- 507 [23] D. Qu, D. Qu, H. Shi, and H. Shi, "Studies of activated carbons used in double-  
508 layer capacitors," *Construction*, pp. 99–107, 1998.
- 509 [24] A. G. Pandolfo and A. F. Hollenkamp, "Carbon properties and their role in  
510 supercapacitor.pdf," *J. Power Sources*, vol. 157, no. 1, pp. 11–27, 2006.
- 511 [25] A. B. Fuertes, F. Pico, and J. M. Rojo, "Influence of pore structure on electric  
512 double-layer capacitance of template mesoporous carbons," *J. Power Sources* ,  
513 vol. 133, no 2, pp. 329–336, 2004.

- [26] E. Frackowiak and F. Béguin, "Carbon materials for the electrochemical storage of energy in capacitors," *Carbon N. Y.*, vol. 39, no. 6, pp. 937–950, 2001.
- [27] S. Lagergren, "About the theory of so-called adsorption of soluble substance," *Kungliga Svenska Vetenskap akademien Handlingar*, vol. 24, pp. 1–39, 1898.
- [28] B. E. Conway, *Electrochemical Supercapacitors-Scientific Fundamentals and Technological Applications*. Publishing: New York, N.Y.: Kluwer Academic / Plenum Publishers, 1999.
- [29] Y. R. Nian and H. Teng, "Influence of surface oxides on the impedance behavior of carbon-based electrochemical capacitors," *J. Electroanal. Chem.*, vol. 540, pp. 119–127, 2003.
- [30] M. A. Adamson, *Physical and Chemistry of Surface*. Publishing: John Wiley & Sons Inc, 1980.
- [31] R. Slimani , A. Anouzla, Y. Abrouki, et al. Removal of a cationic dye -Methylene Blue- from aqueous media by the use of animal bone meal as a new low cost adsorbent. *J Mater Environ Sci*. 2:77–87, 2011 .
- [32] A. Regti, M.R. Laamari, S-E.Stiriba, M. El Haddad. Use of response factorial design for process optimization of basic dye adsorption onto activated carbon derived from Persea species. *Microchem J*, 130:129–36, 2017 .
- [33] Y. Liu Y , Z-W.Wang. Uncertainty of preset-order kinetic equations in description of biosorption data. *Bioresour Technol* 99:3309–12, 2008 .
- [34] A. Özer. Removal of Pb(II) ions from aqueous solutions by sulphuric acid-treated wheat bran. *J Hazard Mater* 141:753–61, 2007 .
- [35] C-I.Lin, L-H.Wang. Rate equations and isotherms for two adsorption models. *J Chin Inst Chem Eng* 39:579–85, 2008 .
- [36] Y. Liu, S-F Yang, H. Xu , K-H Woon, Y-M Lin, J-H Tay . Biosorption kinetics of cadmium(II) on aerobic granular sludge. *Process Biochem* 38:997–1001, 2003.
- [37] G. Alberti, V. Amendola, M. Pesavento, R. Biesuz . Beyond the synthesis of novel solid phases: review on modelling of sorption phenomena. *Coord Chem Rev* 256:28–45, 2012 .
- [38] YS Ho. Review of second-order models for adsorption systems. *J Hazard Mater* 136:681–9, 2006 .

- [39] Y. Liu Y , YJ Liu. Biosorption isotherms, kinetics and thermodynamics. *Sep Purif Technol* 61:229–42, 2008 .
- [40] W. Plazinski, W. Rudzinski, A. Plazinska. Theoretical models of sorption kinetics including a surface reaction mechanism: a review. *Adv Colloid Interface Sci* 152:2–13, 2009.
- [41] K.L. Tan, B.H. Hameed. Insight into the adsorption kinetics models for the removal of contaminants from aqueous solutions. *Journal of the Taiwan Institute of Chemical Engineers* 74 25–48, 2017.
- [42] M. Madhava Rao, A. Ramesh, G. Purna Chandra Rao, and K. Sessaiah, “Removal of copper and cadmium from the aqueous solutions by activated carbon derived from Ceiba pentandra hulls,” *J. Hazard. Mater.*, vol. 129, no. 1–3, pp. 123–129, 2006.
- [43] M. M. Rao, D. K. Ramana, K. Sessaiah, M. C. Wang, and S. W. C. Chien, “Removal of some metal ions by activated carbon prepared from Phaseolus aureus hulls,” *J. Hazard. Mater.*, vol. 166, no. 2–3, pp. 1006–1013, 2009.
- [44] V. C. Srivastava, I. D. Mall, and I. M. Mishra, “Adsorption of toxic metal ions onto activated carbon. Study of sorption behaviour through characterization and kinetics,” *Chem. Eng. Process. Process Intensif.*, vol. 47, no. 8, pp. 1275–1286, 2008.
- [45] J. Acharya, J. N. Sahu, C. R. Mohanty, and B. C. Meikap, “Removal of lead(II) from wastewater by activated carbon developed from Tamarind wood by zinc chloride activation,” *Chem. Eng. J.*, vol. 149, no. 1–3, pp. 249–262, 2009.
- [46] J. Anandkumar and B. Mandal, “Removal of Cr(VI) from aqueous solution using Bael fruit (*Aegle marmelos correa*) shell as an adsorbent,” *J. Hazard. Mater.*, vol. 168, no. 2–3, pp. 633–640, 2009.
- [47] S. Chen, Q. Yue, B. Gao, Q. Li, and X. Xu, “Removal of Cr(VI) from aqueous solution using modified corn stalks: Characteristic, equilibrium, kinetic and thermodynamic study,” *Chem. Eng. J.*, vol. 168, no. 2, pp. 909–917, 2011.
- [48] E. Asuquo, A. Martin, P. Nzerem, F. Siperstein, and X. Fan, “Adsorption of Cd(II) and Pb(II) ions from aqueous solutions using mesoporous activated carbon adsorbent: Equilibrium, kinetics and characterisation studies,” *J. Environ. Chem. Eng.*, vol. 5, no. 1, pp. 679–698, 2017.
- [49] A. Mittal, A. Malviya, D. Kaur, J. Mittal, and L. Kurup, “Studies on the

adsorption kinetics and isotherms for the removal and recovery of Methyl Orange from wastewaters using waste materials,” *J. Hazard. Mater.*, vol. 148, no. 1–2, pp. 229–240, 2007.

[50] Y. Huang, S. Li, J. Chen, X. Zhang, and Y. Chen, “Adsorption of Pb(II) on mesoporous activated carbons fabricated from water hyacinth using H<sub>3</sub>PO<sub>4</sub> activation: Adsorption capacity, kinetic and isotherm studies,” *Appl. Surf. Sci.*, vol. 293, pp. 160–168, 2014.

[51] H. Qiu, L. Lv, B. Pan, Q. Zhang, W. Zhang, and Q. Zhang, “Critical review in adsorption kinetic models,” *J. Zhejiang Univ. A*, vol. 10, no. 5, pp. 716–724, 2009.

**Figure 1. Adapter designed in 3D to be incorporated into a therm**  
[Click here to download high resolution image](#)

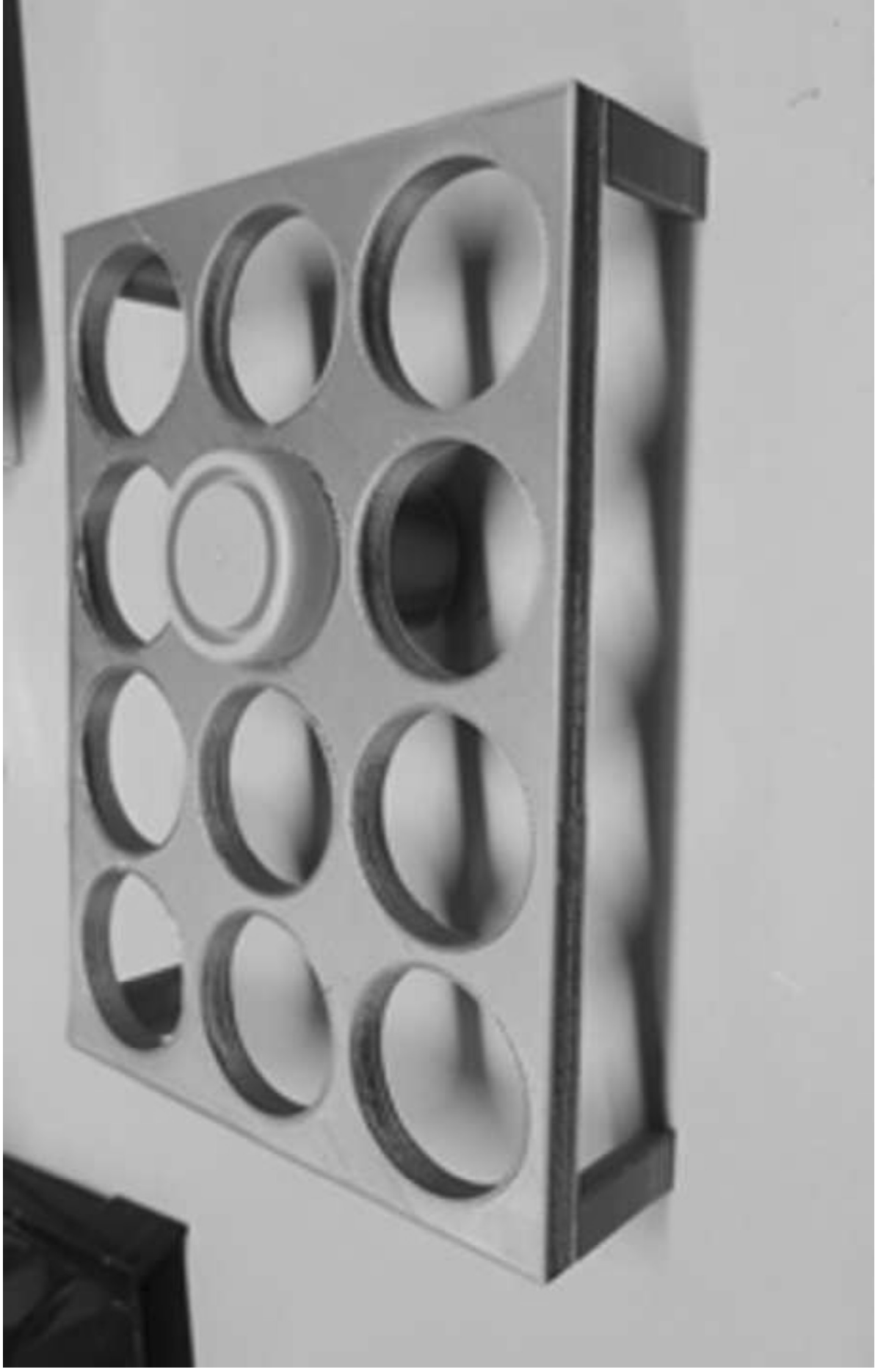


**Figure 2. System of integrated electrodes (designed in 3D).**  
[Click here to download high resolution image](#)

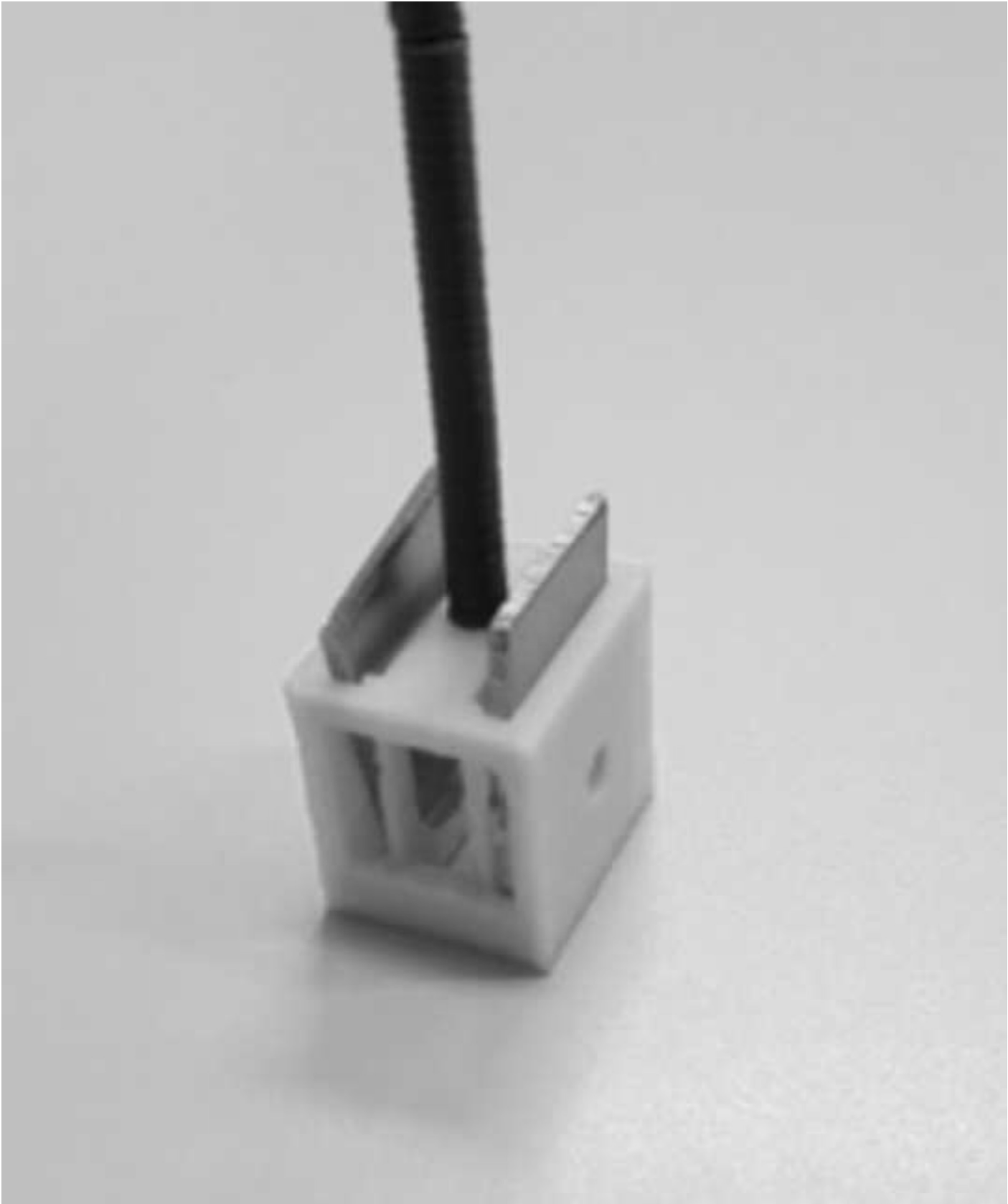


Figure 3. FT-IR spectra for P-T-500 series  
[Click here to download high resolution image](#)

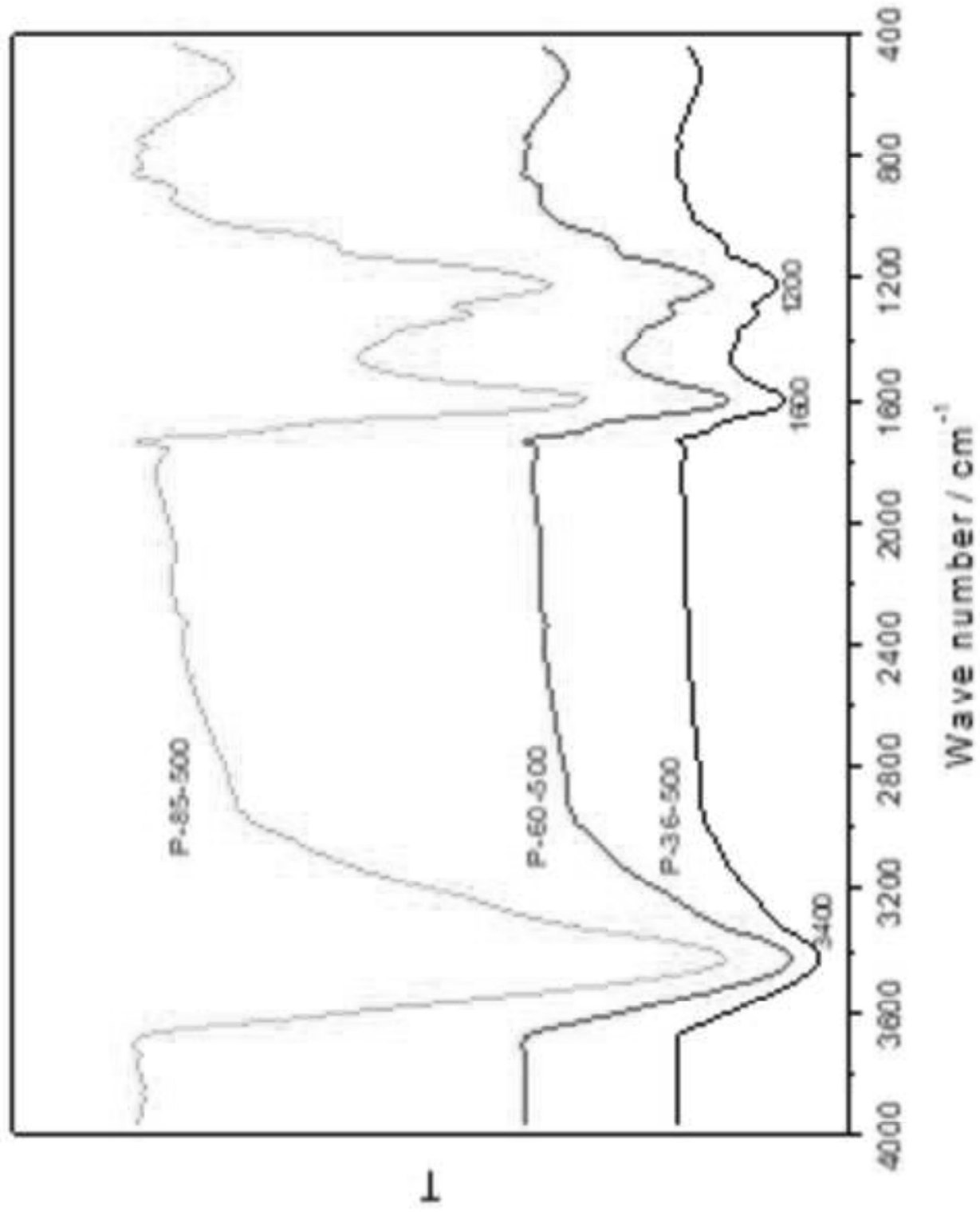


Figure 4 Variation of the electrical conductivity with pressure  
[Click here to download high resolution image](#)

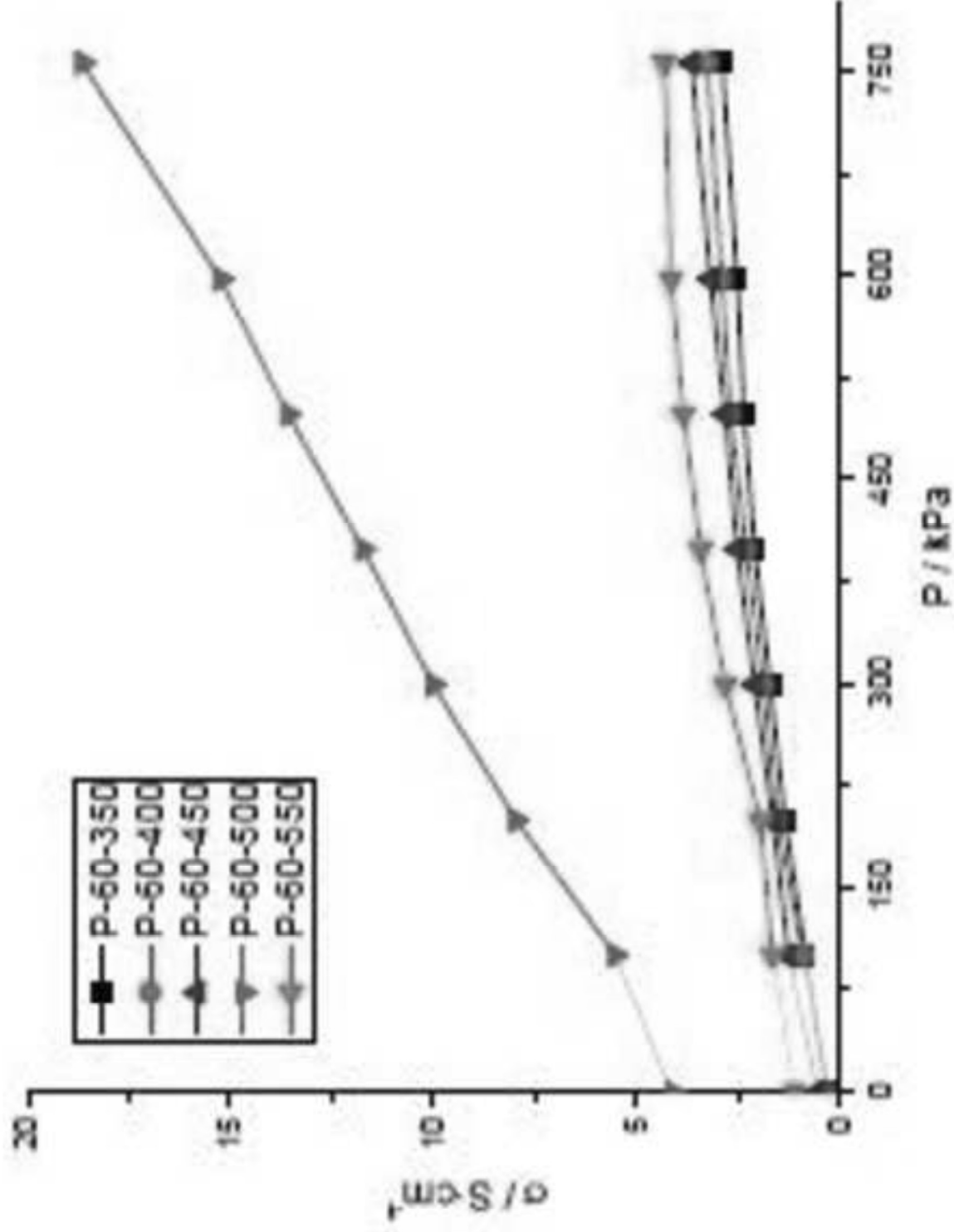


Figure 5. Adsorption and electroadsorption kinetics of the prepa  
[Click here to download high resolution image](#)

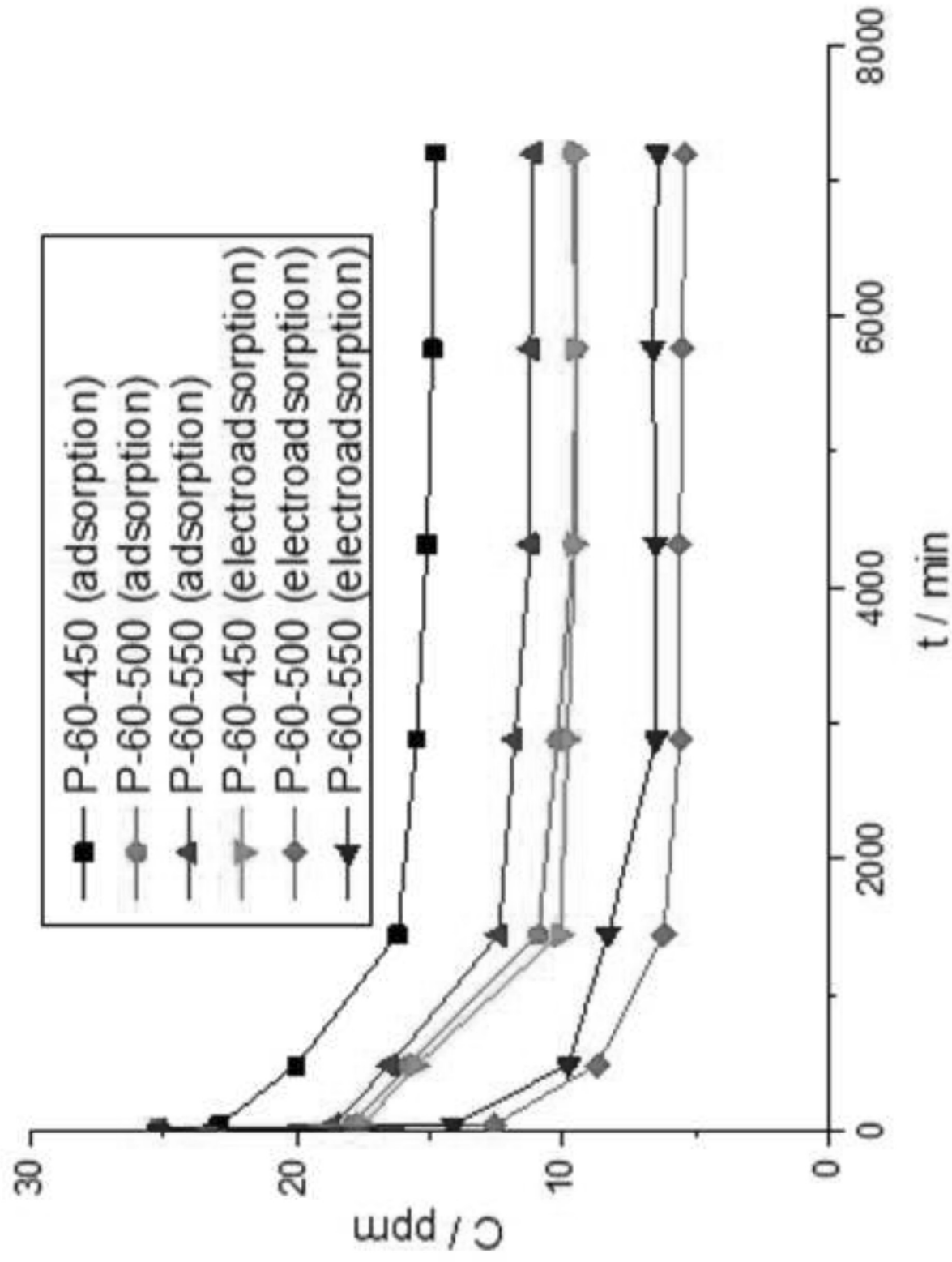


Figure 6. Pseudo-first order model: adsorption (A)  
[Click here to download high resolution image](#)

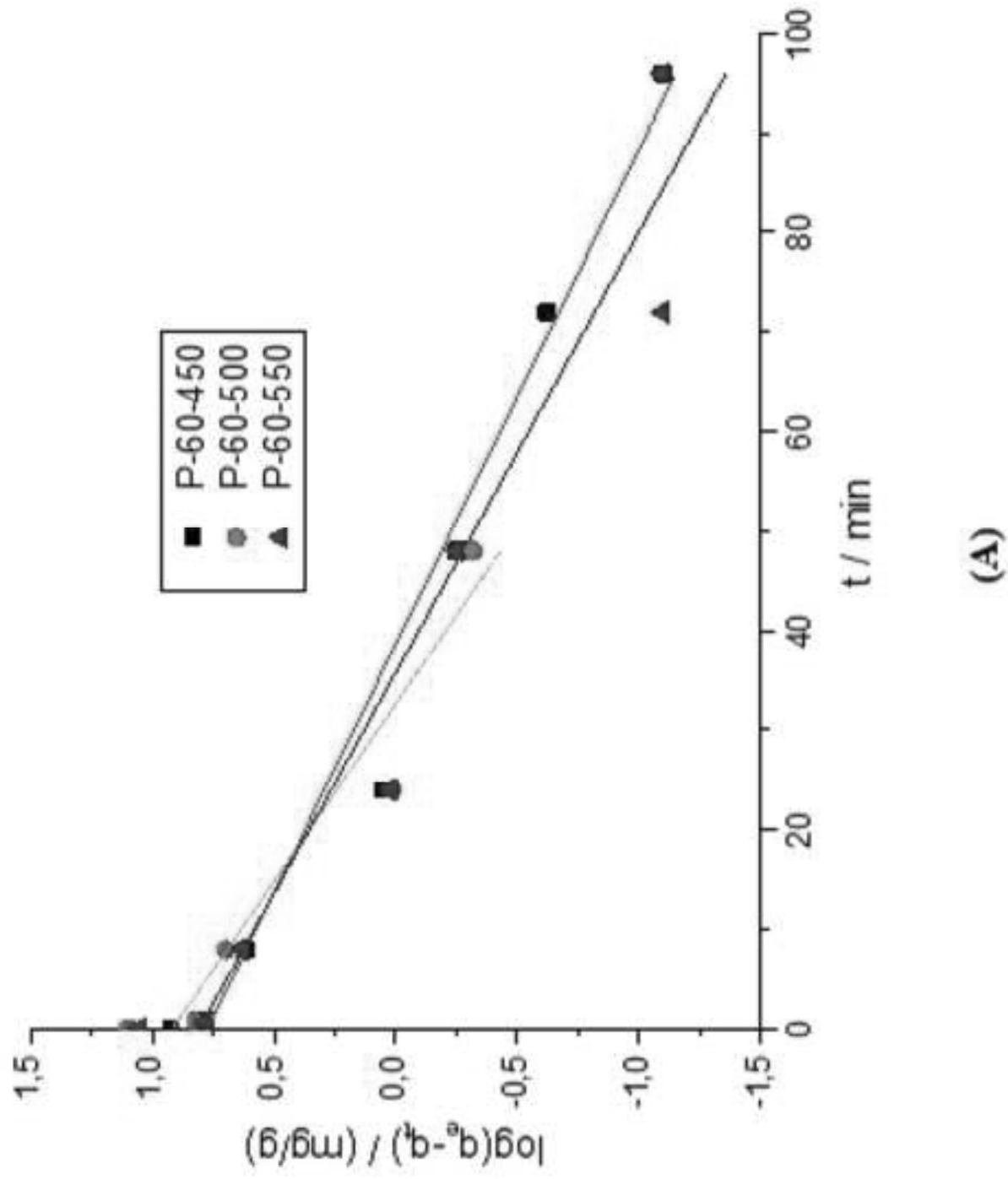


Figure 6. Pseudo-first order model: electroadsorption (B)  
[Click here to download high resolution image](#)

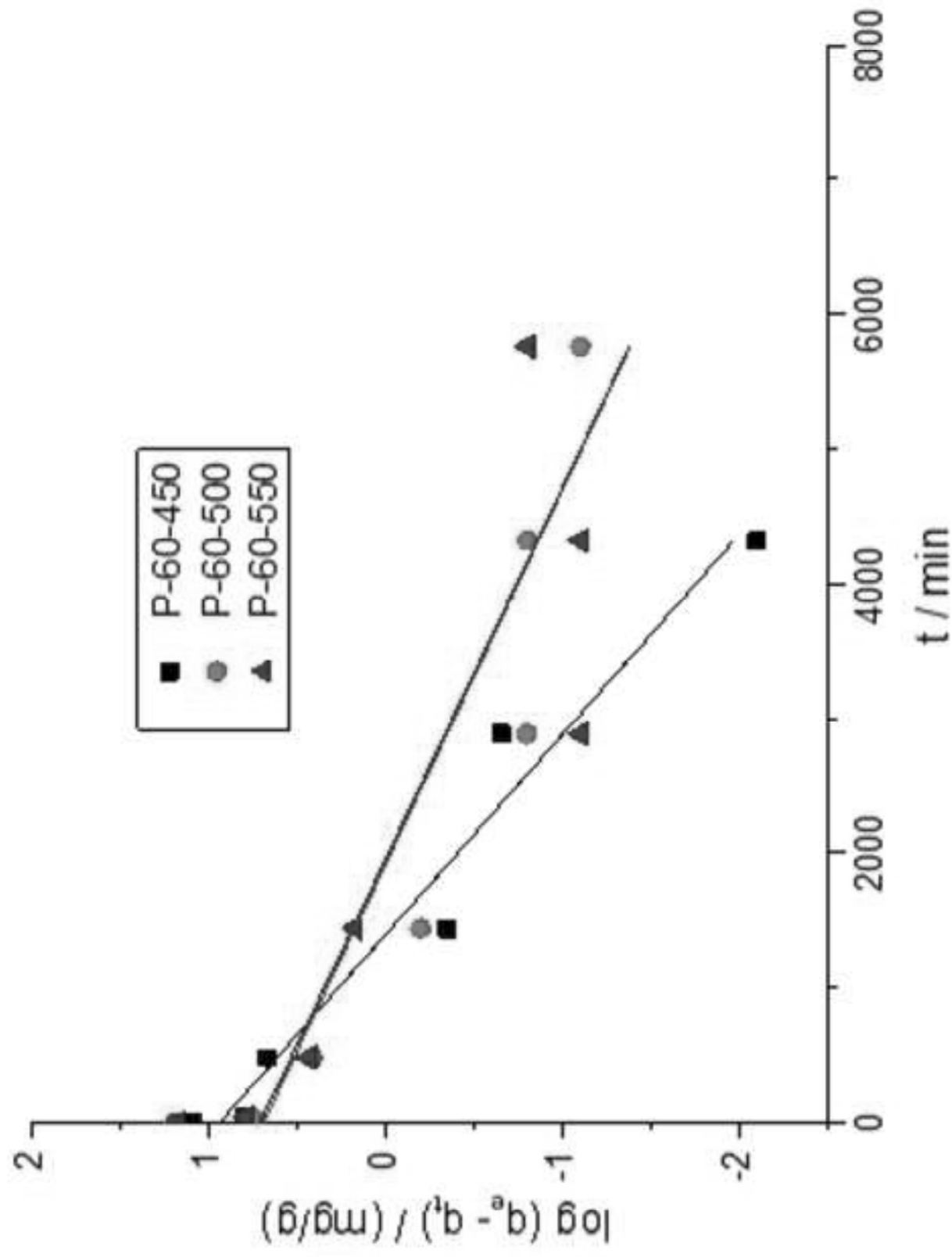


Figure 7: Pseudo-second order model: (A) adsorption  
[Click here to download high resolution image](#)

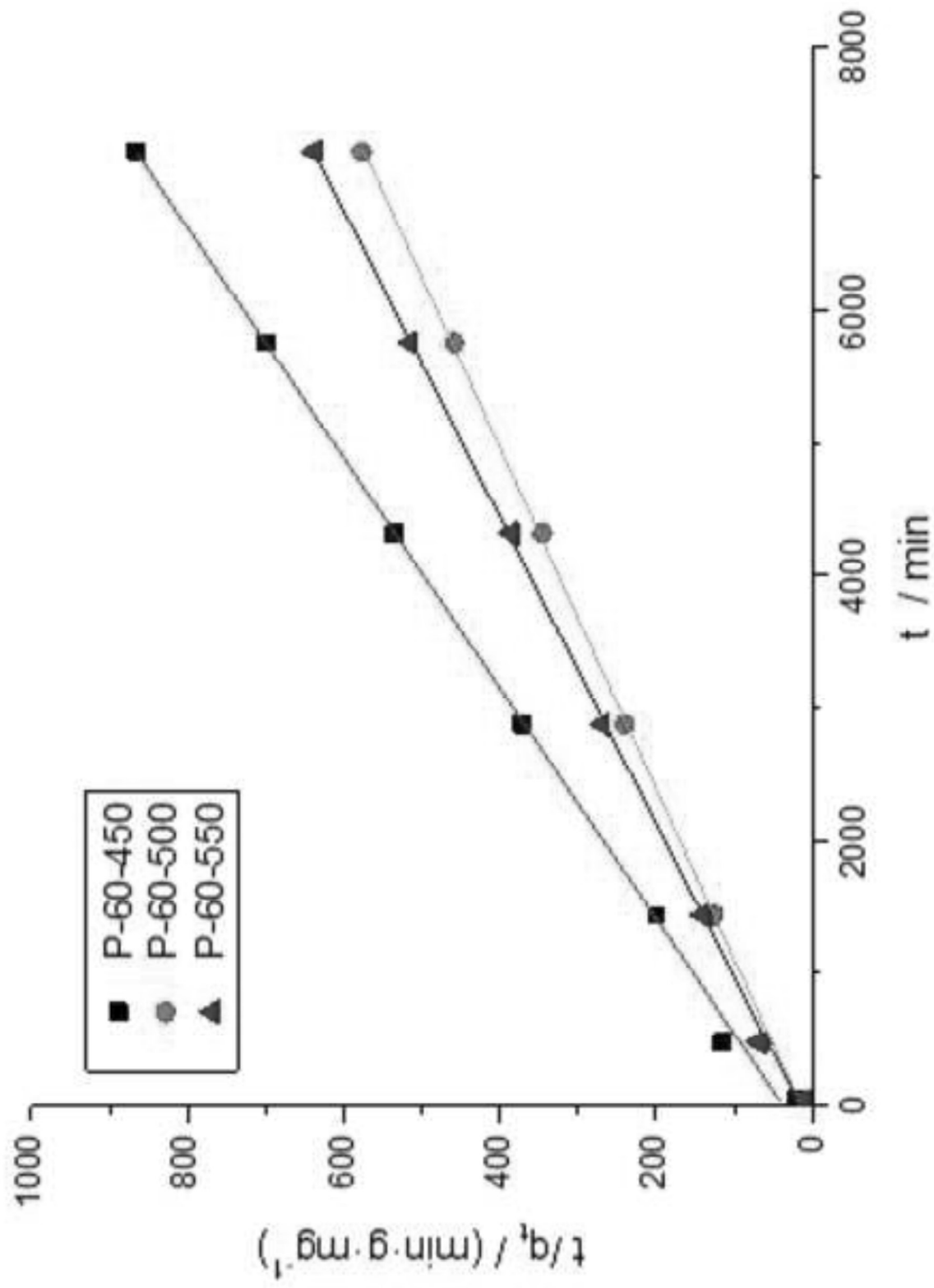


Figure 7: Pseudo-second order model: (B) electro-adsorption  
[Click here to download high resolution image](#)

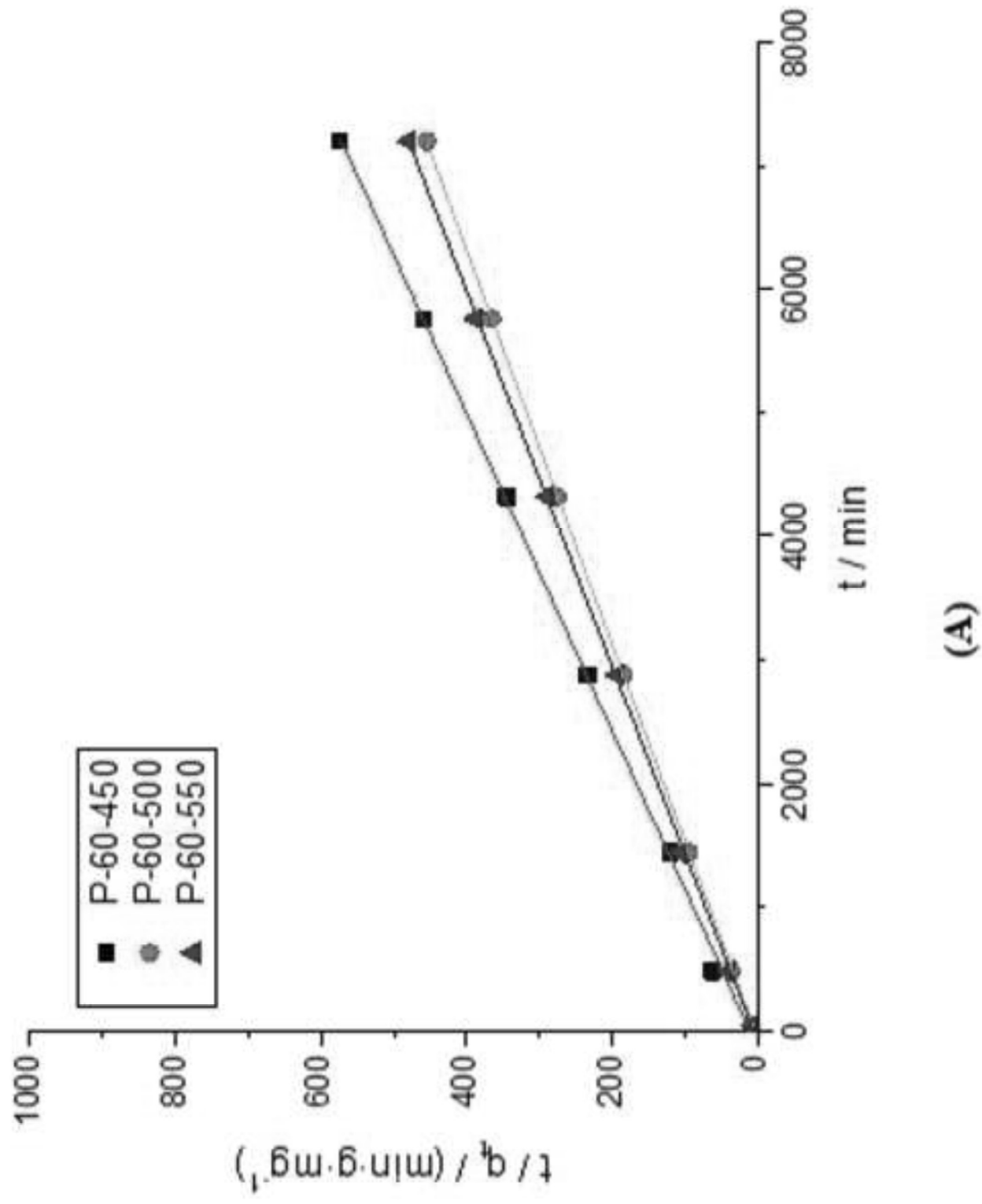


Figure 8: Intraparticle diffusion model: (A) adsorption  
 Click here to download high resolution image

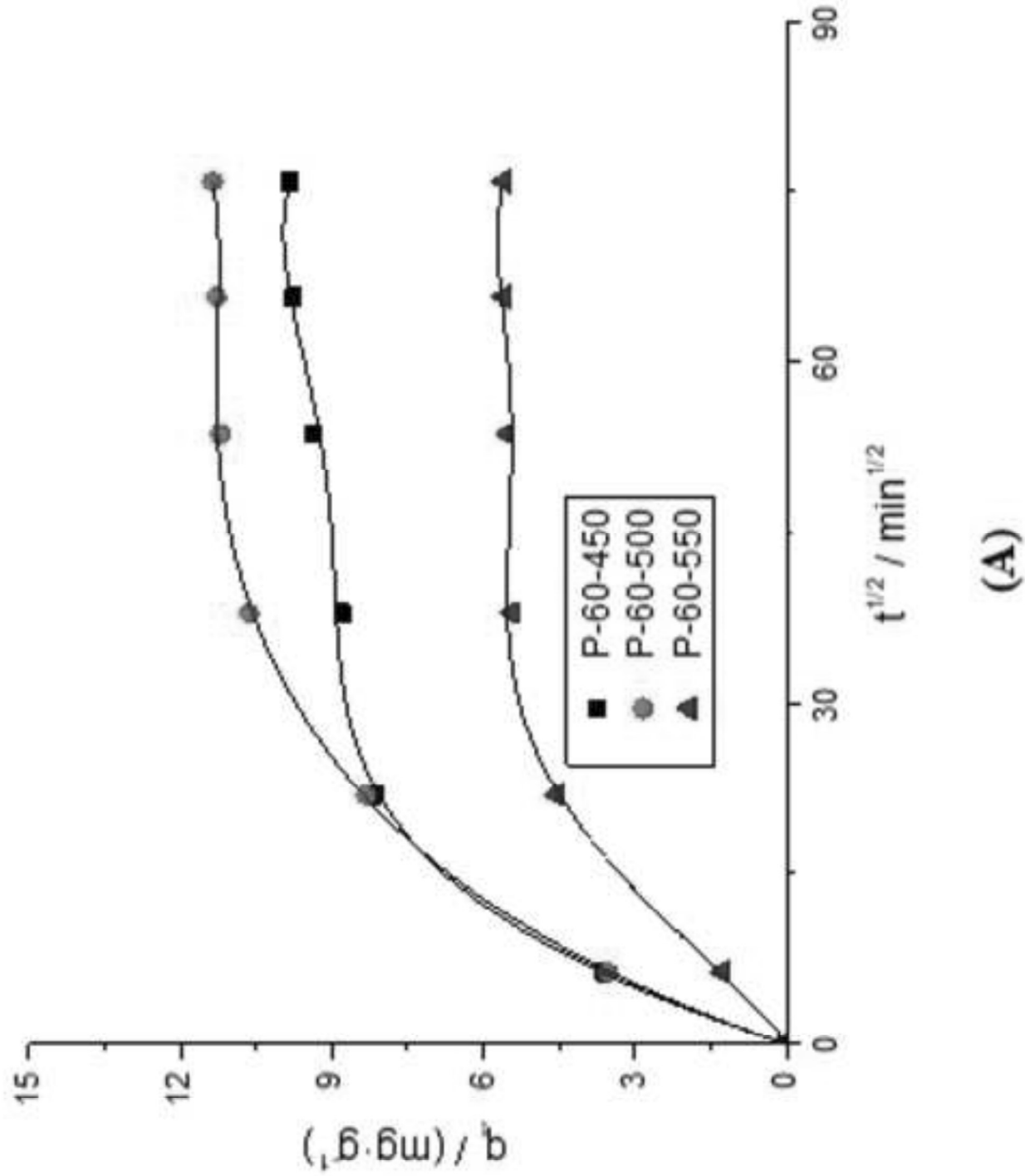


Figure 8: intraparticle diffusion model: (B) electro-adsorption  
 Click here to download high resolution image

